Adsorption (2015) 21:659–669
DOI 10.1007/s10450-015-9716-2

SBA-15 materials: calcination temperature influence on textural properties and total silanol ratio

Reyna Ojeda-López[1] · Isaac J. Pérez-Hermosillo[1] · J. Marcos Esparza-Schulz[1] · Adrián Cervantes-Uribe[2] · Armando Domínguez-Ortiz[1]

Received: 29 August 2015 / Revised: 22 October 2015 / Accepted: 4 November 2015 / Published online: 14 November 2015

Abstract SBA-15 ordered mesoporous materials were synthesized using the method reported by Zhao et al. (Science 279:548–552, 1998a). This study seeks to determine the calcination temperature influence on texture and chemical properties of SBA-15 materials. In the present work, materials calcined at 523, 623, 723, 823 and 923 K were studied. The hexagonal structure of these solids was characterized by powder X-ray diffraction (XRD) and transmission electron microscopy. Textural properties were assessed by nitrogen adsorption. The chemical species in materials were determined by nuclear magnetic resonance and fourier transform infrared pyridine (pyridine-FTIR). The results obtained indicate that calcination at 623 K is enough to promote both, the total silanol ratio and superficial specific area. Afterward, materials calcined at 623 and 823 K were functionalized with APTES molecules via "grafting" method. Next, materials texture was characterized by nitrogen adsorption. Finally, their CO_2 adsorption capacity was also evaluated. Material calcined at 623 K and amine-functionalized showed the higher CO_2 adsorption capacity.

Keywords Adsorption · Amine-functionalization · APTES · Calcination · SBA-15 · Silanol

✉ Armando Domínguez-Ortiz
doar@xanum.uam.mx

[1] Departamento de Química, Universidad Autónoma Metropolitana–Iztapalapa, P.O. Box 55-534, Col. Vicentina, Av. San Rafael Atlixco 186, 09340 México, DF, Mexico

[2] Universidad Juárez Autónoma de Tabasco, DACB, P.O. Box 24, Km 1 Carretera Cunduacán-Jalpa de Méndez, 86690 Cunduacán, TAB, Mexico

1 Introduction

In recent years, ordered mesoporous materials (MMO) SBA-15 have been studied intensely, (Zhao et al. 2000; Zhao et al. 1998a, b), due to their numerous applications as catalysts and adsorbents, among others (Bronnimann et al. 1988; Van Grieken et al. 2003; Iler 1979; Landmesser et al. 1994; Melero et al. 2002). This material, c.f. Fig. 1, consists of a silicon oxide matrix (silica), whose main characteristics are: (1) pore size between 2 and 50 nm, i.e. mesopores according to IUPAC (Sing et al. 1985), (2) cylindrical mesopores having a hexagonal arrangement, (3) presence of micropores (pore size <2 nm), mesopores channels are interconnected through micropores, and (4) significant surface chemical activity (Van Der Voort et al. 1991), this is a function of concentration and distribution, on the solid surface, of different silanol and siloxano groups (Peng et al. 2009; Sneh and George 1995; Zaborski et al. 1989; Zhuravlev 2000); notably silanol groups enable the "anchor" of various chemical compounds and thus may modify the surface of the solid for specific applications (Calleja et al. 2011; Liu et al. 2002; Wang et al. 2006). The methodology to synthetized SBA-15 materials involves three stages: (1) hydrolysis-condensation of silicate species (TEOS) around the micelles of surfactant (Pluronic 123), (2) consolidation of solid matrix under hydrothermal conditions, and (3) material calcination to remove surfactant residues. Materials obtained by this route are mesoporous solids with high thermal and mechanical stability. They present silanol groups on their surface and the amount of these is a function of calcination temperature. Finally, these materials get an easy accessibility to their porosity.

SBA-15 materials have two different chemical groups on their surface (Legrand 1998; Vansant et al. 1995), viz

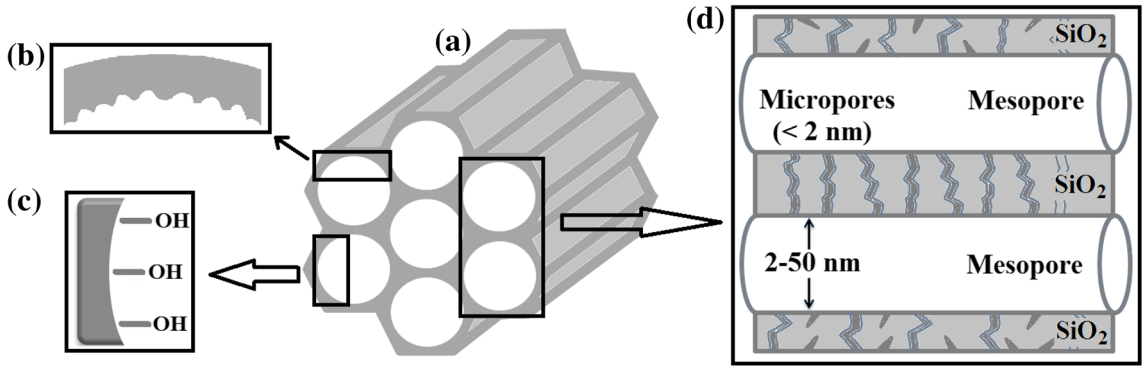

Fig. 1 The main SBA-15 characteristics: **a** hexagonal arrange of cylindrical mesopores, **b** pore surface roughness, **c** superficial silanol groups, and **d** mesopores are interconnected by micropores

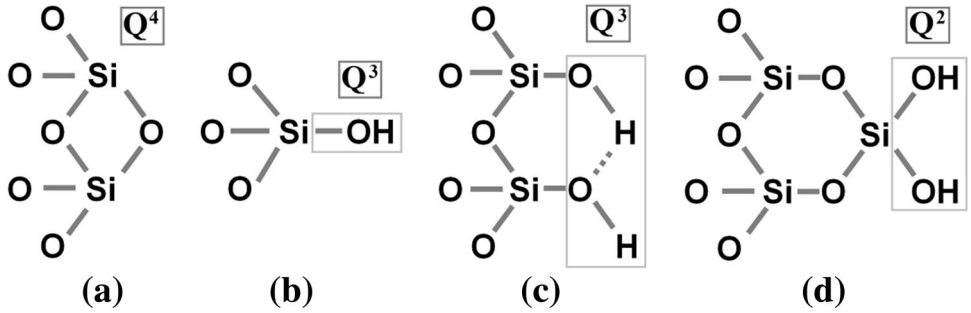

Fig. 2 Chemical composition of silica surface: **a** siloxane group, **b** isolated or free silanol group, **c** vicinal or bridged silanol group, and **d** geminal silanol group

Fig. 2: (1) hydrophobic siloxane group (≡Si–O–Si≡) and (2) hydrophilic silanol group (≡Si–OH). Silanol groups are partitioned in:

- *Isolated* (or free silanols), there a surface silicon atom is linked to three O–Si and one –OH,
- *Vicinal* (or bridged silanols), there two silanol groups are attached by hydrogen bridge, and
- *Geminal*, they consist of two silanol groups attached to one silicon atom.

The discovery of silanol groups on silica surface and their quantification (α_{OH}, number of hydroxyl groups per nm^2 or silanol number) is attributed to Kiselev (1936). Kiselev and Lygin (1975) have stated that geminal silanols probably do not exist on a dry surface, but Knözinger et al. (1988) used high-resolution FTIR to make the reasonable statement that even the very small band at 3746 cm^{-1} is a superposition of a "single free" and a "single geminal" hydroxyl band. Zhuravlev (1987) compared more than 100 amorphous silica samples (silica gels, aerogels, porous glasses) and he concluded that concentration of hydroxyl groups α_{OH} is independent of the origin and structural characteristics as: specific surface area, type of the pores, size distribution of the pores, and particle packing density; then α_{OH} value is considered as a physicochemical constant.

Van Der Voort et al. (1991) studied three different types of silica gel (Kieselgel 40, 60, and 100) with varied pore distributions and they concluded that the relative distribution of free and bridged silanol groups on silica gel surface is a function of calcination temperature. Besides, accessibility and reactivity of free silanol groups are not affected by sample porosity. When, during the synthesis, temperature rises in both, condensation and calcination processes, the formation of siloxane group occurs via condensation of silanol groups (Hench and West 1990). Siloxane constitutes the main part of solid matrix. Observe that two silanol groups condensation yields one siloxane group (viz Fig. 3).

Silanol groups on silica surface allow the chemical "anchorage" of diverse functional chemical groups (Liu et al. 2002; Wang et al. 2006). Notably, materials SBA-15 amine-functionalized have presented interesting CO_2 storage capacity and good regeneration (Chao et al. 2013; Sanz et al. 2013; Vilarrasa-García et al. 2014; Patil et al. 2012; Wang et al. 2007; Yan et al. 2011). SBA-15 materials have been functionalized by grafting method. In this method, there is a covalent bond between an organosilane precursor of organic chain and silanol groups (Van Grieken et al. 2003; Zhao and Lu 1998). The functionalizing agent was (3-aminopropyl)triethoxysilane (APTES). Figure 4 illustrates the mechanism of SBA-15 functionalization, where the amine may join one, two or three OH groups.

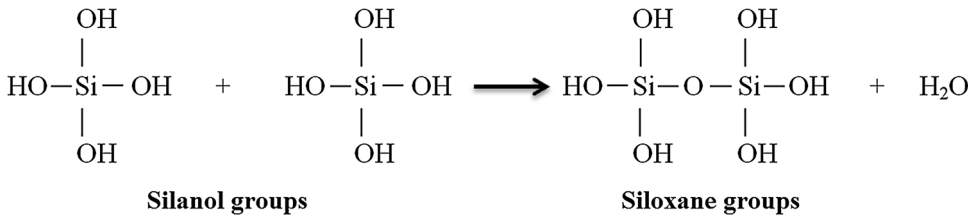

Fig. 3 Two silanol groups condensation to generate one siloxane

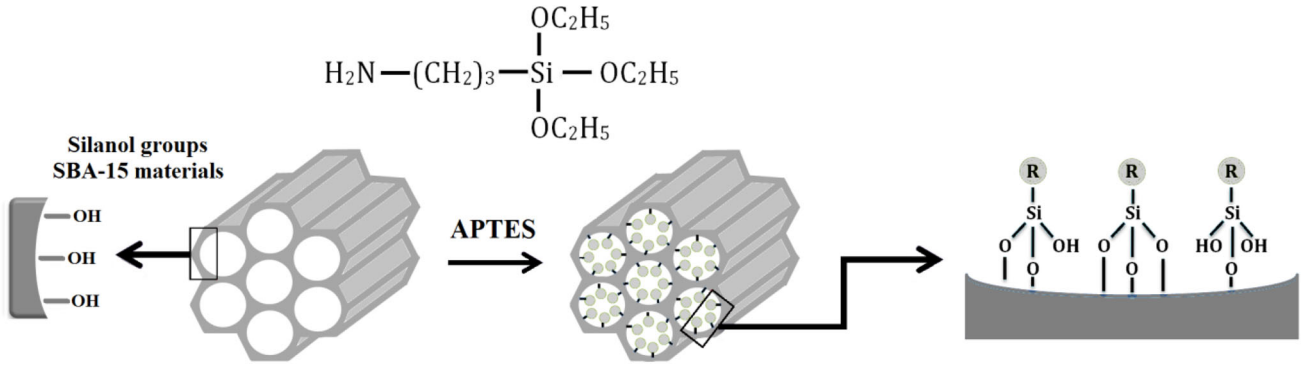

Fig. 4 Mechanism of SBA-15 functionalization with APTES

The aims of this work are:

(1) To evaluate the effect of temperature during the calcination processes, in order to find the better temperature to maximize both, the total ratio silanol and the elimination surfactant residues.
(2) To assess the influence of the functionalization on textural properties of SBA-15 materials.
(3) To explore the CO_2 adsorption capacity of SBA-15 materials amine-functionalized.

2 Materials and methods

2.1 Materials

Tetraethyl orthosilicate (TEOS, 98 %, Aldrich), surfactant poly (ethylene glycol)-block-poly-(propyleneglycol)-block-poly(ethylene glycol) (P123, Aldrich), (3-amino-propyl) triethoxysilane (APTES, 99 %, Aldrich), hydrochloric acid (36.5–38 %, J.T. Baker) and absolute ethanol (EtOH, 99.9 %, Baker) were used as received.

2.2 Experimental development

The preparation of pure silica SBA-15 samples was similar to method reported by Zhao et al. (1998a, b). 4.0 g of triblock copolymer Pluronic P-123 was dissolved with stirring in a solution of 120 g of deionized water and 24 g of HCl 36.5–38 %, until full dissolution. Next it was performed dropwise addition of 8.5 g of TEOS. The resulting mixture was stirred at 313 K for 20 h and then the solution was aged at 353 K for 2 days under static condition. The prepared sample was recovered by filtration with 150 mL of ethanol and air-dried at 363 K for 24 h. The organic template was removed by calcination at different temperatures (523, 623, 723, 823 y 923 K) in a tube furnace. During calcination process, temperature went up 1 K per minute until the desired temperature was reached, after that temperature was constant for 4 h.

SBA-15 materials were functionalized with APTES following the next sequential procedure: (1) 0.40 g of SBA-15 was heating under vacuum at 373 K for 12 h to remove residual water, (2) SBA-15 was added in 50 mL of ethanol with vigorous stirring, (3) 3.03 g of APTES (13.7 mmol) was added to previous mixture, (4) the mixture was stirred at 353 K for 24 h under nitrogen atmosphere, and finally (5) the sample was washed with ethanol and dried at 373 K for 20 h.

2.3 Characterization techniques

Powder XRD patterns were recorded on a Bruker D8 Advance, using monochromatic CuKα radiation with a wavelength of 1.54 Å in the low angle region (0.6° to 5.0° in the 2θ scale). This technique gives parameters as pore

diameter, wall thickness, and the uniformity of cylindrical pores hexagonal array. TEM technique was used to determine the internal structure of SBA-15 materials, showing hexagonal structure and pore size. The analysis was performed on a High-resolution Transmission Electron Microscopy, HRTEM Jeol 2100F, using as a light source a field emitter and 200 kV acceleration.

Textural properties of samples were determined by nitrogen adsorption. The measurements were performed with a Micromeritics ASAP 2020 system at liquid nitrogen temperature (77 K). Before measurement, SBA-15 sample was degassed at 373 K for 12 h. The specific surface area of solid samples were calculated by multiple-point Brunauer–Emmett–Teller (BET) method in the relative pressure range of $P/P^0 = 0.05–0.25$ (Brunauer et al. 1938). Pore size distribution curves were computed by using the non-local density functional theory (NLDFT) method (Ravikovitch and Neimark 2001). Nuclear magnetic resonance (NMR) was used to obtain the total ratio silanol on solid surface. It was performed ^{29}Si nuclear magnetic resonance (NMR) in a Bruker Advace II300 spectrometer operating at 59.62 MHz for ^{29}Si. The ^{29}Si was recorded by magic angle spinning (MAS) at 5 kHz. The ^{29}Si NMR spectra were referenced to tetramethylsilane. To determine the acidic nature of the materials FTIR-Pyridine was used. Using this technique provides acid sites concentration and type (Lewis and Brönsted). The equipment used for this analysis was a Nicolet Avatar 320 FTIR spectrometer. Finally, CO_2 adsorption isotherms were obtained on a Quantachrome Autosorb-1 equipment, at 283 K at pressures from 0.001 to 1 bar. Samples were outgassed at 283 K for 12 h under vacuum.

3 Results and discussion

3.1 Results from nitrogen adsorption

Figure 5a shows the nitrogen adsorption isotherms of SBA-15 materials calcined at 523(C-523), 623(C-623), 723(C-723), 823(C-823) y 923(C-923) K. The expressions in parenthesis correspond to sample calcination temperature. Note that the obtained isotherms are type IV with hysteresis loop H1 (Sing et al. 1985). Samples C-523 and C-623 present the more important nitrogen adsorption. When the material is calcined at temperatures bigger than 623 K, there is abrupt down of nitrogen adsorption volume, this is due to partial sinterization of the material (Ojeda-López et al. 2014). Nevertheless, observe that the width of the hysteresis loop did not change significantly after calcination at 623 K, this means preservation of pores arrangement (Fig. 5a, boxes on the top left).

Thermal degradation of P123 surfactant occurs between 500 and 600 K (Kao et al. 2005). However, calcination conditions in silica are clearly different. Observe that the nitrogen isotherm of sample C-523 presents a small inclination, it is due to an incomplete elimination of surfactant residues, i.e. existence of organic fragment in pores, producing pore size dispersion. In contrast, for calcination temperatures ≥623 K isotherms present uniform hysteresis, i.e. a pores size distribution with poor dispersion. As observed in Fig. 5b, where NLDFT curve for sample C-523 is the widest, with pore diameters from 5.8 to 9.0 nm. When calcination temperature rises, it is observed a mean pore size diminution (a displacement toward left), it means a pore size diminution. Notice also that micropores

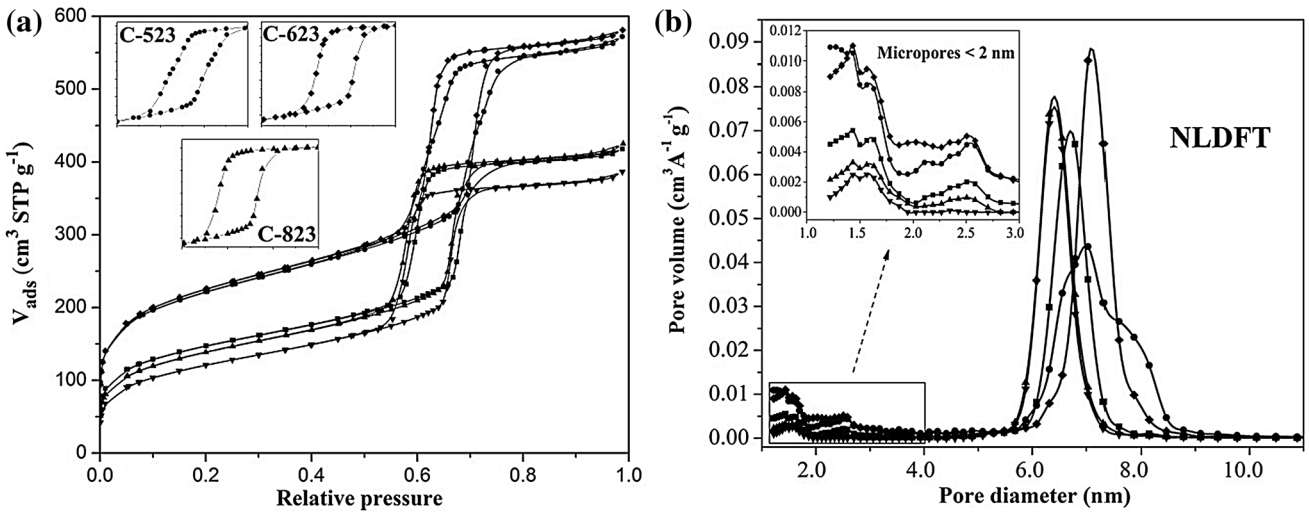

Fig. 5 Nitrogen adsorption on SBA-15 materials: **a** adsorption isotherms and **b** NLDFT model pore size distributions. C-523 (*black circle*), C-623 (*black diamond*), C-723 (*black square*), C-823 (*black up-pointing triangle*), and C-923 (*black down-pointing triangle*)

population decreases when calcination temperature increases (c.f. square in Fig. 5b).

In Table 1, textural properties of SBA-15 materials, gotten from nitrogen adsorption, are presented. Observe that sample NC (no calcined), has less surface area than samples C-523 and C-623, this is due to presence of surfactant residues in pores. The maximum value of surface area is reached when calcination temperature is 623 K (sample C-623). For higher calcination temperatures, a decreasing of surface area follows, that is caused by sinterization phenomenon. Pore size distribution ($D_{P(NLDFT)}$) follows a similar behavior.

3.2 Results from ^{29}Si NMR

In NMR spectroscopy ^{29}Si, silanol groups are denoted as "Q" sites, siloxane bridges are called "Q^4 sites", single silanols (isolated and vicinal) "Q^3 sites" and geminal silanols "Q^2 sites" (Legrand 1998; Vansant et al. 1995; La Vars et al. 2013), please c.f. Fig. 2.

Figure 6a presents NMR spectra ^{29}Si by direct polarization with high power decoupling (HPDEC) for SBA-15 materials. The samples NC and C-523 have clearly the three signals: Q^2 (germinal silanols), Q^3 (free and vicinal silanols), and Q^4 (siloxane); while in the spectrum corresponding to sample C-623, signals Q^2 and Q^3 are less intense and the signal Q^4 is stronger, this indicates an important silanol groups condensation. In samples C-723, C-823 and C-923 spectra, signals Q^2 and Q^3 fade and signal Q^4 is clearly observed, this indicates that most of the silanol groups have reacted to form siloxane bonds.

Figure 6b shows NMR spectra {^{1}H} ^{29}Si by cross polarization—the magic angle spinning (CP-MAS). Unlike the spectra obtained by HPDEC, in this case each silicon

Table 1 Textural properties of SBA-15 materials

Sample	S_{BET} ($m^2\ g^{-1}$)	V_{MICRO} ($cm^3\ g^{-1}$)	V_{MESO} ($cm^3\ g^{-1}$)	V_T ($cm^3\ g^{-1}$)	$Dp_{(NLDFT)}$ (nm)
NC	676	0.031	0.854	0.886	8.15
C-523	763	0.091	0.729	0.819	7.05
C-623	776	0.095	0.754	0.848	7.05
C-723	516	0.042	0.540	0.582	6.80
C-823	486	0.019	0.571	0.590	6.60
C-923	428	0.012	0.524	0.536	6.60

S_{BET} BET specific surface area, V_{MICRO} microporous volume, V_{MESO} mesoporus volumen, V_T total pore volume, $D_{p(NLFDT)}$ average pore diameter by NLDFT

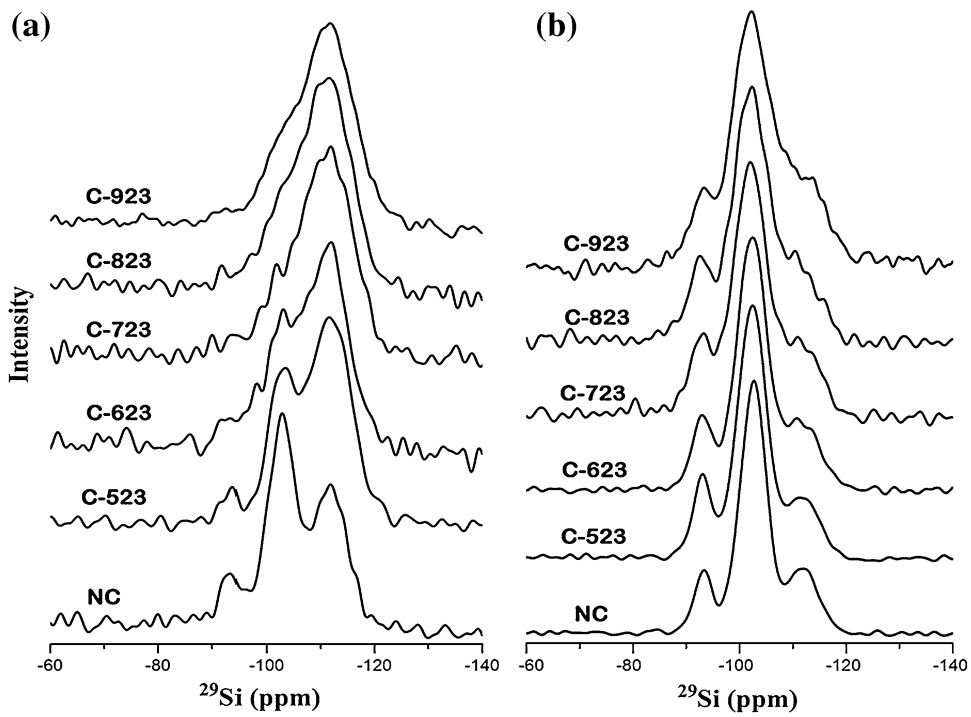

Fig. 6 Spectrum SBA-15: **a** ^{29}Si HPDEC NMR and **b** CP–MAS {^{1}H} ^{29}Si NMR

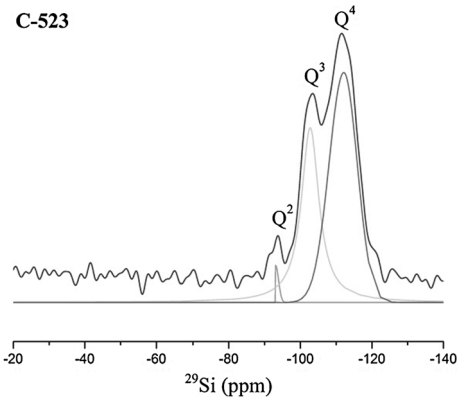

Fig. 7 The allocation of the Q^2, Q^3 and Q^4 site on the NMR spectrum of sample C-523

atom provides a characteristic signal in function of its connection degree (cross-linking) with a neighbor hydrogen atom. In principle signal Q^4 should not be observed, since siloxane groups do not have hydrogen atoms in their structure; however a small Q^4 signal is observed, this is due to some hydrogen atoms, belonging to silanol groups or water molecules, in the neighborhood of siloxane groups interacting with them. Observe below that signal Q^2 decreases and signal Q^3 grows when calcination temperature increases, these behaviors are due to significant changes in solids structure, e.g. temperature calcination above 923 K produces porous structure collapse and sinterization of SBA-15 materials, as observed in adsorption results section and Ojeda et al. (2014).

Figure 7 presents the deconvolution of signals Q^2, Q^3 y Q^4, in spectrum MAS ^{29}Si NMR, corresponding to sample C-523. The spectrum was deconvoluted to obtain the corresponding area of each specie, total area represent the total silicon species (Ide et al. 2013). This allows determinate the relative amount of each specie. Measured quantities are presented in Table 2.

In columns 1 and 2 are given the ratio $Q^3/(Q^2 + Q^3)$, corresponding to single silanol/total silanols and the ratio $2Q^2/(Q^3 + Q^4)$ corresponding to geminal silanols/total silanols, respectively. Notice that there is no relation between previous ratios and calcination temperature. In column three, values of $(2Q^2 + Q^3)/(Q^2 + Q^3 + Q^4)$, denote the total SiOH ratio. Observe that these values decrease as calcination temperature increases (0.66 in sample NC to 0.17 in sample C-923), this behavior is due to condensation reactions are favored by calcination temperature rise. It also produces a more compact matrix, which causes the decreasing of all textural properties, as indicated by values in column 4, where condensation degree $(Q^4/Q^2 + Q^3 + Q^4)$ increases from 0.43 to 0.74.

3.3 Results from ^{13}C CP–MAS NMR

Spectra ^{13}C NMR corresponding to samples NC and C-623 are presented in Fig. 8. The goal of this analysis was to evaluate the removal of residues from surfactant molecules (P123). These residues must be removed to liberate pores. Note in NC spectrum the signals at 15, 70 and 76 ppm, they correspond to organic residues; while in C-623 spectrum this signals was not observed, indicating the absence of surfactant residues. In brief, in prepared SBA-15 materials, carbon atoms from surfactant molecules are not chemisorbed to SiO_2 matrix, allowing a good removal of surfactant residues by calcination at 623 K.

It is pertinent to mention that in the majority of published work relative to SBA-15 materials, calcination happens between 773 and 823 K (Chong and Zhao 2003; Esparza et al. 2004; Ojeda et al. 2003). Results presented in previous Sects. (3.1–3.2) of this manuscript signal that sample calcined at 623 K presents the highest surface area (please c.f. Table 1) and a good removal of surfactant residues (viz Fig. 8). This corroborates the results of Benamor et al. 2012, they performed a similar study about SiO_2 materials, concluding that calcination at 573 K is the best one to remove the template and preserve both, structural properties and silanol content. Next, results of C-623 sample are presented and contrasted with results of C-823 sample, i.e. a system normally reported in the literature.

3.4 Results from FTIR pyridine

Pyridine spectra of samples C-623 and C-823 are given in Fig. 9. Results of adsorption of pyridine show clearly two

Table 2 Q^2, Q^3 and Q^4 species in SBA-15 materials

	$SiO_3(OH)$ $Q^3/(Q^3 + Q^2)$	$SiO_2(OH)$ $2Q^2/(Q^3 + Q^2)$	Total SiOH ratio $(2Q^2 + Q^3)/(Q^2 + Q^3 + Q^4)$	Condensation degree $Q^4/(Q^2 + Q^3 + Q^4)$
NC	0.86	0.14	0.66	0.43
C-523	0.82	0.18	0.50	0.58
C-623	0.81	0.19	0.45	0.62
C-723	0.84	0.16	0.39	0.66
C-823	0.83	0.17	0.38	0.67
C-923	0.91	0.10	0.17	0.74

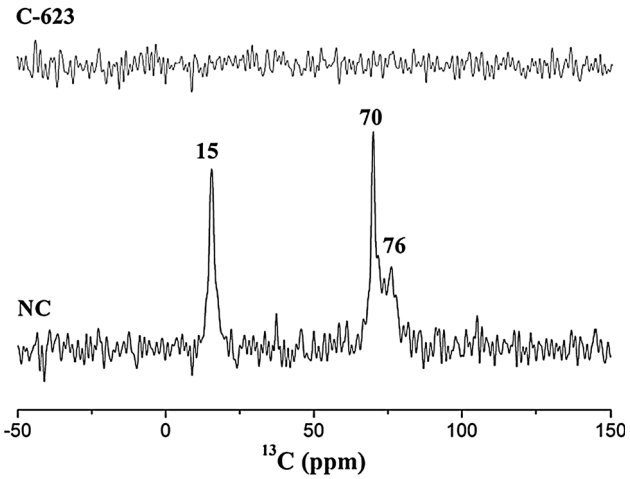

Fig. 8 Spectra ^{13}C CP–MAS NMR samples NC and C-623

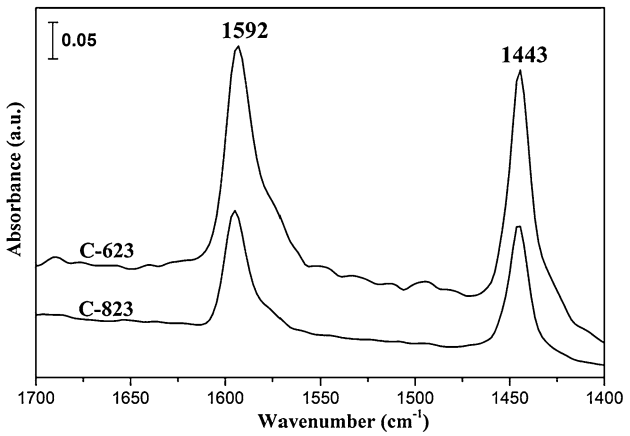

Fig. 9 FTIR pyridine spectra

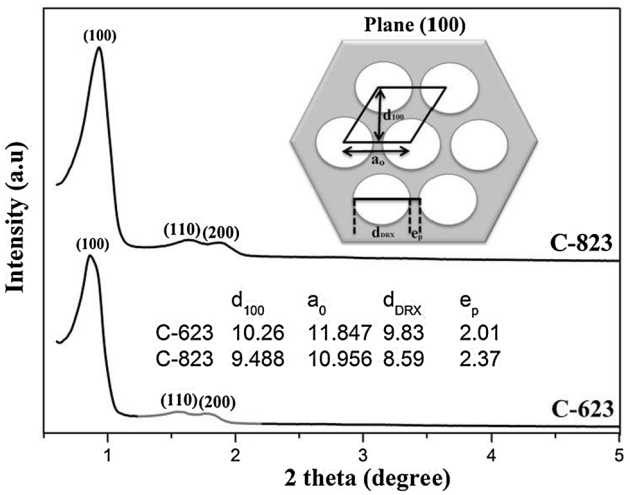

Fig. 10 Powder XRD diffraction patterns of SBA-15 materials. d_{100} interplanar distance plane (100), a_o distance between centers of two adjacent pores, d_{DRX} XRD pore diameter, e_p wall thickness between adjacent pores

signals at wavenumbers 1443 and 1592 cm^{-1}, they correspond to bond formation between pyridine and hydrogen atom belonging to silanol group. This kind of interaction is one pyridine to one OH and it is known as H-bonded Py (HPy) (Zaki et al. 2001). The foremost difference between spectra is absorption intensity is that a more important absorption is observed for C-623 sample. Therefore, C-623 sample has a bigger amount of surface OH groups than C-823 sample.

3.5 Results from XRD

Diffractograms of SBA-15 materials calcined at 623 and 823 K are presented in Fig. 10. Observe that both materials have three peaks associated to refraction planes (100), (110), and (200). These peaks indicate a hexagonal arrangement of cylindrical mesopores, the characteristic structure of SBA-15 materials. Various geometrical parameters of mesopores hexagonal arrangement in the plane (100) are also shown. Following Kruk et al. (2003), the thickness of the pore walls, e_p, was calculated. These values are also giving in Fig. 10. Notice that when calcination temperature grows the value of e_p increases and interplanar distance, d_{100}, goes down. These results corroborate the decline of average pore size that was observed by nitrogen adsorption (please c.f. Table 1).

3.6 Results from TEM

Figure 11 shows images TEM of SBA-15 materials calcined at 623 and 823 K. The two-dimensional p6 mm hexagonal symmetry, characteristic SBA-15 materials, can be seen on both samples. Pore diameter estimated from TEM image is in good agreement with analogous diameter estimated from NLDFT adsorption isotherm. For C-623 sample, TEM gives 7.4 versus 7.0 nm given by NLDFT. For C-823 sample, TEM gives 7.1 versus 6.6 nm given by NLDFT.

3.7 Results from CO_2

In this section is studied the CO_2 adsorption capacity of SBA-15 materials calcined at 623 and 823 K and then amine-functionalized whit APTES using "grafting" method, early described. First the amine-functionalized samples C-623-APTES and C-823-APTES were studied by nitrogen adsorption in order to characterize their texture. Figure 12a presents nitrogen adsorption isotherms of these materials, and Table 3 gives pore diameter and specific surface area obtained from preceding isotherms. The surface area of C-623-APTES is a half of C-623 surface area. A similar behavior is observed for C-823-APTES, surface area decreases 40 % with respect to surface area of C-823.

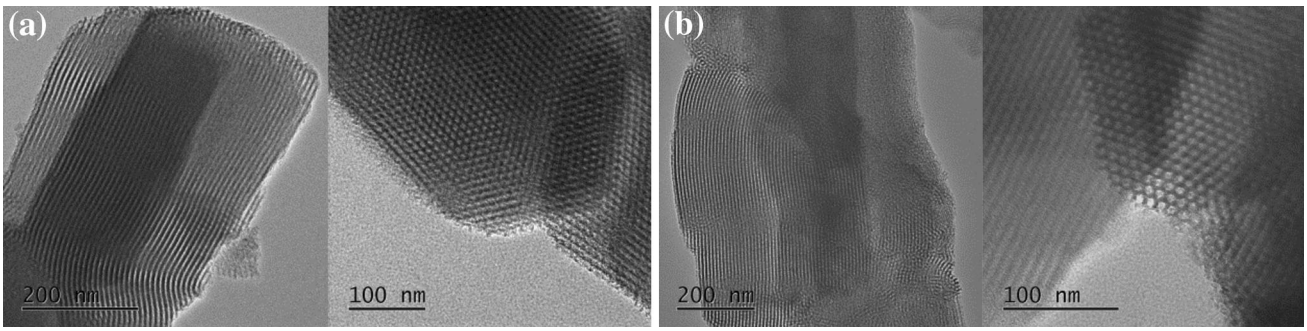

Fig. 11 TEM images corresponding to **a** C-623 and **b** C-823

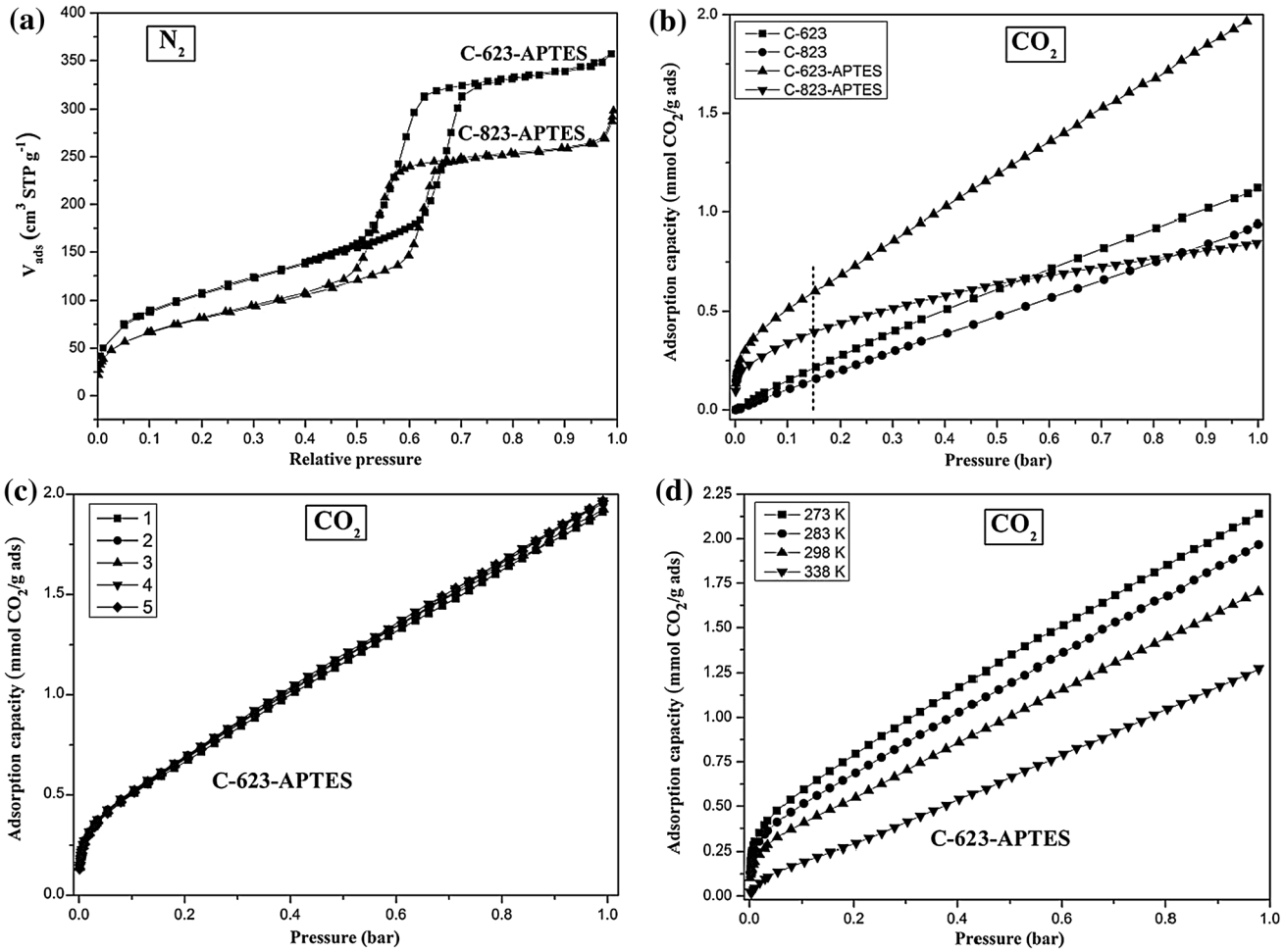

Fig. 12 Isotherms of SBA-15 amine-functionalized materials: **a** nitrogen adsorption, **b** CO_2 adsorption at 283 K **c** regenerability at 283 K on C-623-APTES, and **d** CO_2 adsorption at 273, 283, 298, and 338 K

The diminution of mean pore size for amine-functionalized materials was 0.7 nm, this due to anchoring of APTES molecules on mesopores walls. It is known that the approximate size of APTES molecule varies between 0.6 and 1.0 nm (Chong et al. 2004; Savino et al. 2011).

Finally, these samples were analyzed by CO_2 adsorption at 283 K (viz Fig. 12b). In this analysis at 1 bar pressure, the amount of CO_2 adsorbed was 1.96 and 0.85 mmol/g for C-623-APTES and C-823-APTES, respectively, i.e. C-623-APTES exhibits a better CO_2 adsorption than C-823-

Table 3 Textural properties SBA-15 amine-functionalized

	S_{BET} (m^2 g^{-1})	$D_{P(NLDFT)}$ (nm)
C-623	776	7.0
C-623-APTES	392	6.3
C-823	486	6.6
C-823-APTES	296	5.9

APTES. This could be due to combined effects of a better functionalization (higher total silanol ratio) and bigger surface area of C-623 material with respect to C-823 material.

At low CO_2 pressure, both isotherms (C-623-APTES and C-823-APTES) are nearly vertical lines, indicating a strong interaction between amine group and the CO_2 molecule (Danon et al. 2011). The isotherms of non-functionalized materials (C-523 and C-823) are also presented in Fig. 12b. Note that, under similar conditions, non-functionalized materials adsorb significantly less than functionalized materials. For example, at 0.15 bar and 283 K, C-623-APTES adsorbs 0.6 mmol/g and C-623 adsorbs 0.15 mmol/g; whereas, under the same conditions, C-823-APTES adsorbs 0.4 mmol/g and C-823 adsorbs 0.21 mmol/g. This behavior could be due to a very weak interaction between CO_2 molecules and silanol groups (Roque-Malherbe et al. 2010).

These materials could have an industrial utility in CO_2 capturing. For that it is important to evaluate both, CO_2 adsorption capacity and regenerability of material. The typical composition of a gaseous industrial effluent is 15 % in volume of CO_2, if an ideal behavior is considered, the partial pressure of CO_2 would be 0.15 bar (Yuan et al. 2014). Observe on Fig. 12b, at 0.15 bar, the amount of adsorbed gas was 0.60 mmol/g for C-623-APTES, 68 % more than C-823-APTES (0.4 mmol/g). By other hand, regenerability was evaluated by CO_2 adsorption on C-623-APTES, five adsorption isotherms were performed one after the other. The adsorbent was pretreated under vacuum at 373 K for 6 h, before to make each isotherm to remove all the surface adsorbents such as H_2O and CO_2. Figure 12c shows the five adsorption isotherms performed consecutively. Note no significant changes between the different isotherms, signaling a good material reversibility.

Finally, Fig. 12d shows the adsorption capacity of CO_2 on C-623-APTES material, at four different temperatures (273, 283, 298, and 338 K). Note that temperature rise causes a decrease CO_2 total volume adsorbed (under 1 bar of CO_2). At 0.15 bar and 298 K the material has an adsorption capacity of 0.48 mmol/g, which decrease to 0.24 mmol/g at 338 K. While the total volume adsorbed at 298 K is 1.71 mmol/g and 1.3 mmol/g at 338 K. Notice that these values are higher than the values reported by Wang et al. 2007, i.e. 1.18 mmol/g (1 bar, 298 K) and 0.95 mmol/g (1 bar, 338 K) for a material SBA-15 functionalized with APTES.

4 Conclusions

The main conclusions of this experimental work are:

(1) The material calcined at 623 K presented the greatest total silanol ratio and an efficient removal of surfactant residues.
(2) The best calcination temperature is 623 K, if one wants facilitate amine-functionalized.
(3) The comparison between CO_2 adsorption by C-623-APTES and C-823-APTES materials shows that CO_2 adsorption is more efficient on first one.

Acknowledgments We thank at the Consejo Nacional de Ciencia y Tecnología (CONACyT) for the support granted for the development of this work. To the network SEP-PROMEP "Diseño Nanoscópico y Textural de Materiales Avanzados", with the Project "Síntesis y Fisicoquímica de Materiales Mesoporosos" (UAM-I CA-31 Fisicoquímica de Superficies)". Our thanks to Laboratories of DRX (INFR-2011-1-163250), Resonancia Magnética Nuclear and the Microscopia Electronica de Transmisión of the Universidad Autónoma Metropolitana-Iztapalapa.

References

Benamor, T., Michelin, L., Lebeau, B., Marichal, C.: Flash induction calcination: a powerful tool for total template removal and fine tuning of the hydrophobic/hydrophilic balance in SBA-15 type silica mesoporous materials. Microporous Mesoporous Mater. **147**, 334–342 (2012)

Bronnimann, C.E., Zeigler, R.C., Maciel, G.E.: Proton NMR study of dehydration of the silica gel surface. J. Am. Chem. Soc. **110**, 2023–2026 (1988)

Brunauer, S., Emmett, P.H., Teller, E.: Adsorption of gases in multimolecular layers. J. Am. Chem. Soc. **60**, 309–319 (1938)

Calleja, G., Sanz, R., Arencibia, A., Sanz-Pérez, E.S.: Influence of drying conditions on amine-functionalized SBA-15 as adsorbent of CO2. Top. Catal. **54**, 135–145 (2011)

Chao, K.J., Klinthong, W., Tan, C.S.: CO2 adsorption ability and thermal stability of amines supported on mesoporous silica SBA-15 and fumed silica. J. Chin. Chem. Soc. **60**, 735–744 (2013)

Chong, A.S.M., Zhao, X.S.: Functionalization of SBA-15 with APTES and characterization of functionalized materials. J. Phys. Chem. B. **107**, 12650–12657 (2003)

Chong, A.S.M., Zhao, X.S., Kustedjo, A.T., Qiao, S.Z.: Functionalization of large-pore mesoporous silicas with organosilanes by direct synthesis. Microporous Mesoporous Mater. **72**, 33–42 (2004)

Danon, A., Stair, P.C., Weitz, E.: FTIR study of CO2 adsorption on amine-grafted SBA-15: elucidation of adsorbed species. J. Phys. Chem. C **115**, 11540–11549 (2011)

Esparza, J.M., Ojeda, M.L., Campero, A., Domínguez, A., Kornhauser, I., Rojas, F., Vidales, A.M., López, R.H., Zgrablich, G.: N2 sorption scanning behavior of SBA-15 porous substrates. Colloids Surf. A Physicochem. Eng. Asp. **241**, 35–45 (2004)

Van Grieken, R., Calleja, G., Stucky, G.D., Melero, J.A., García, R.A., Iglesias, J.: Supercritical fluid extraction of a nonionic surfactant template from SBA-15 materials and consequences on the porous structure. Langmuir **19**, 3966–3973 (2003)

Hench, L.L., West, J.K.: The Sol-Gel Process. Chem. Rev. **90**, 33–72 (1990)

Ide, M., El-Roz, M., De Canck, E., Vicente, A., Planckaert, T., Bogaerts, T., Van Driessche, I., Lynen, F., Van Speybroeck, V., Thybault-Starzyk, F., Van Der Voort, P.: Quantification of silanol sites for the most common mesoporous ordered silicas and organosilicas: total versus accessible silanols. Phys. Chem. Chem. Phys. **15**, 642–650 (2013)

Iler, R.K.: The Chemistry of Silica: Solubility, Polymerisation, Colloid and Surface Properties and Biochemistry. Wiley, New York (1979)

Kao, H.M., Chen, C.L., Chiao, S.W.: Solid polymer plectrolyte pased on pluronic P123 triblock copolymer-siloxane organic—inorganic hybrid. J. Chin. Chem. Soc. **52**, 693–699 (2005)

Kiselev, A.V.: Kiselev, A.V. (17).pdf. Kollodn. Zh. 2, 17 (1936)

Kiselev, A.V., Lygin, V.I.: Infrared Spectra of Surface Compounds. Wiley, New York (1975)

Knözinger, E., Hoffmann, P., Echterhoff, R.: Surface and adsorption studies of high surface area oxides. Mikrochim. Acta. II **95**, 27–33 (1988)

Kruk, M., Jaroniec, M., Joo, S.H., Ryoo, R.: Characterization of regular and plugged SBA-15 silicas by using adsorption and inverse carbon replication and explanation of the plug formation mechanism. J. Phys. Chem. B. **107**, 2205–2213 (2003)

La Vars, S.M., Johnston, M.R., Hayles, J., Gascooke, J.R., Brown, M.H., Leterme, S.C., Ellis, A.V.: 29Si{1H} CP-MAS NMR comparison and ATR-FTIR spectroscopic analysis of the diatoms Chaetoceros muelleri and *Thalassiosira pseudonana* grown at different salinities. Anal. Bioanal. Chem. **405**, 3359–3365 (2013)

Landmesser, H., Kosslick, H., Storek, W., Fricke, R.: Interior surface hydroxyl groups in ordered mesoporous silicates. Solid **101–103**, 271–277 (1994)

Legrand, A.P.: The Surface Properties of Silicas. Wiley, France (1998)

Liu, Y., Lee, J.Y., Hong, L.: Functionalized SiO2 in poly (ethylene oxide)-based polymer electrolytes. J. Power Sources **109**, 507–514 (2002)

Melero, J.A., Stucky, G.D., Van Grieken, R., Morales, G.: Direct syntheses of ordered SBA-15 mesoporous materials containing arenesulfonic acid groups. J. Mater. Chem. **12**, 1664–1670 (2002)

Ojeda, M.L., Esparza, J.M., Campero, A., Cordero, S., Kornhauser, I., Rojas, F.: On comparing BJH and NLDFT pore-size distributions determined from N2 sorption on SBA-15 substrata. Phys. Chem. Chem. Phys. **5**, 1859–1866 (2003)

Ojeda-López, R., Pérez-Hermosillo, I.J., Esparza-Schulz, J.M., Domínguez-Ortiz, A.: Efecto de la temperatura de calcinación sobre la concentración de grupos silanoles en superficies de SiO2 (SBA-15). Av. en Química **9**, 21–28 (2014)

Patil, U., Fihri, A., Emwas, A.-H., Polshettiwar, V.: Silicon oxynitrides of KCC-1, SBA-15 and MCM-41 for CO2 capture with excellent stability and regenerability. Chem. Sci. **3**, 2224–2229 (2012)

Peng, L., Qisui, W., Xi, L., Chaocan, Z.: Investigation of the states of water and OH groups on the surface of silica. Colloids Surf A Physicochem. Eng. Asp. **334**, 112–115 (2009)

Ravikovitch, P.I., Neimark, A.V.: Characterization of micro- and mesoporosity in SBA-15 materials from adsorption data by the NLDFT method. J. Phys. Chem. B. **105**, 6817–6823 (2001)

Roque-Malherbe, R., Polanco-Estrella, R., Marquez-Linares, F.: Study of the interaction between silica surfaces and the carbon dioxide molecule. J. Phys. Chem. C **114**, 17773–17787 (2010)

Sanz, R., Calleja, G., Arencibia, A., Sanz-Perez, E.S.: Development of high efficiency adsorbents for CO2 capture based on a double-functionalization method of grafting and impregnation. J. Mater. Chem. A. **1**, 1956–1962 (2013)

Savino, R., Casadonte, F., Terracciano, R.: In mesopore protein digestion: a new forthcoming strategy in proteomics. Molecules **16**, 5938–5962 (2011)

Sing, K.S.W., Everett, D.H., Haul, R.A.W., Moscou, L., Pierotti, R.A., Rouquérol, J., Siemieniewska, T.: Reporting physisorption data for gas/solid systems with special seference to the setermination of surface srea and sorosity. Pure Appl. Chem. **57**, 603–619 (1985)

Sneh, O., George, S.M.: Thermal stability of hydroxyl groups on a well-defined silica surface. J. Phys. Chem. **99**, 4639–4647 (1995)

Vansant, E.F., Van Der Voort, P., Vrancken, K.C.: Characterization and chemical modification of the silica surface, studies. In: Delmon, B., Yates, J.T. (eds.) Surface Science and Catalysis. vol. 93, Part I. Elsevier, Amsterdam (1995)

Vilarrasa-García, E., Cecilia, J.A., Santos, S.M.L., Cavalcante, C.L., Jiménez-Jiménez, J., Azevedo, D.C.S., Rodríguez-Castellón, E.: CO2 adsorption on APTES functionalized mesocellular foams obtained from mesoporous silicas. Microporous Mesoporous Mater. **187**, 125–134 (2014)

Van Der Voort, P., Gillis-D'Hamers, I., Vrancken, K.C., Vansant, E.F.: Effect of porosity on the distribution and reactivity of hydroxyl groups on the surface of silica gel. J. Chem. Soc. Faraday Trans. **87**, 3899 (1991)

Wang, L., Ma, L., Wang, A., Liu, Q., Zhang, T.: CO2 adsorption on SBA-15 modified by aminosilane. Chin. J. Catal. **28**, 805–810 (2007)

Wang, X.L., Mei, A., Li, M., Lin, Y., Nan, C.W.: Effect of silane-functionalized mesoporous silica SBA-15 on performance of PEO-based composite polymer electrolytes. Solid State Ionics **177**, 1287–1291 (2006)

Yan, X., Zhang, L., Zhang, Y., Yang, G., Yan, Z.: Amine-modified SBA-15: effect of pore structure on the performance for CO_2 capture. Ind. Eng. Chem. Res. **50**, 3220–3226 (2011)

Yuan, M.H., Wang, L., Yang, R.T.: Glow discharge plasma-assisted template removal of SBA-15 at ambient temperature for high surface area, high silanol density, and enhanced CO2 adsorption capacity. Langmuir **30**, 8124–8130 (2014)

Zaborski, M., Vidal, A., Ligner, G., Balard, H., Papirer, E., Burneau, A.: Comparative study of the surface hydroxyl groups of gumed and precipitated silicas. 1. Grafting and chemical characterization. Langmuir **5**, 447–451 (1989)

Zaki, M.I., Hasan, M.A., Al-Sagheer, F.A., Pasupulety, L.: In situ FTIR spectra of pyridine adsorbed on SiO_2-Al_2O_3, TiO_2, ZrO_2 and CeO_2: general considerations for the identification of acid sites on surfaces of finely divided metal oxides. Colloids Surf. A Physicochem. Eng. Asp. **190**, 261–274 (2001)

Zhao, D., Feng, J., Huo, Q., Melosh, N., Fredrickson, G.H., Chmelka, B.F., Stucky, G.D.: Triblock copolymer syntheses of mesoporous silica with seriodic 50 to 300 angstrom pores. Science **279**, 548–552 (1998a)

Zhao, D., Huo, Q., Feng, J., Chmelka, B.F., Stucky, G.D.: Nonionic triblock and star diblock copolymer and oligomeric surfactant syntheses of highly ordered, hydrothermally stable, mesoporous silica structures. J. Am. Chem. Soc. **120**, 6024–6036 (1998b)

Zhao, D., Sun, J., Li, Q., Stucky, G.D., Barbara, S.: Morphological control of highly ordered mesoporous silica SBA-15. Chem. Mater. **12**, 275–279 (2000)

Zhao, X.S., Lu, G.Q.: Modification of MCM-41 by surface silylation with trimethylchlorosilane and adsorption study. J. Phys. Chem. B. **102**, 1556–1561 (1998)

Zhuravlev, L.T.: Concentration of hydroxyl-groups on the surface of amorphous silicas. Langmuir **3**, 316–318 (1987)

Zhuravlev, L.T.: The surface chemistry of amorphous silica. Colloids Surf. **173**, 1–38 (2000)